Switched Control of Three-Phase Voltage Source PWM Rectifier Under a Wide-Range Rapidly Varying Active Load

Wei Zhang, Yanze Hou, Xinbo Liu, and Yuanjun Zhou

***Abstract*—The aircraft electric actuator is one of the most important kind of electric loads of the future more electric aircraft. The power characteristic of an aircraft electric actuator possesses the feature of rapidly varying in a wide range, and it shows constant power load nature in the small-signal sense. In this paper, a novel dc-bus voltage switched control method of three-phase voltage source pulsewidth-modulated rectifiers (VSRs), which aims to solve the problem of flexible voltage regulating under dynamic loads, is proposed under a cascade structure in rotating synchronous coordinates $d-q$. Several linear controllers are designed on different operating points of the VSR, and one controller is implemented on the VSR system according to certain switching law. The stability of the proposed control approach is guaranteed based on the common Lyapunov function method. Simulation and experimental results show that the desired control performance is obtained in the voltage regulating of a VSR with wide-range rapidly varying load. Compared with a classical *PI* controller, the derived switched controller can achieve a considerable reduction in the dip of the dc-bus voltage and a certain reduction in the overshoot of the dc-bus voltage during the control process under an aircraft electric actuator load.**

***Index Terms*—AC motor drives, ac–dc power conversion, power conversion, power conversion harmonics.**

I. Introduction

THREE-PHASE voltage source pulsewidth-modulated (PWM) rectifiers (VSRs) possess many attractive features, such as high power factor, nearly sinusoidal input current, and bidirectional power flow ability [1], [2]. VSRs are increasingly utilized as substitutes for traditional diode rectifiers and phase-controlled rectifiers. Although they are widely used and studied in many industrial applications nowadays, seldom applications have appeared in the aviation industry. As more electric aircraft (MEA) becoming the main trend for future aircrafts, there exists a sharp increase of electric loads in the aircraft power system [3]. The aircraft electric actuator is one of the most important loads of the future MEA and all electric aircraft power grid [4]. It is a position-servo system that shoulders the task of driving the aircraft control surfaces. Unlike the general electric loads, the aircraft actuators behave as constant power loads (CPLs). In addition, during an action process of an aircraft actuator, the input power would vary rapidly within a wide range. These load characteristics bring significant challenges to the power source. The advanced PWM rectifiers play an important role in these aspects, due to more and more attention paid to the power quality and energy efficiency of the aircraft power grid. Therefore, a further investigation on the VSRs is quite important for the aviation industry [5], especially under an electric actuator load.

Extensive studies on the control of VSRs for desired performances have been reported in the past decades [6]–[24]. The results in controller design can be briefly classified into two categories: linear design and nonlinear design. The classical voltage-oriented control in rotating coordinates [6]–[10], which is a linear design method, becomes a standard solution in industrial applications [25]. However, with a linear controller, both the stability and the performance of a VSR cannot be guaranteed under a wide-range rapidly varying load [26]. Nonlinear control strategies have been extensively studied in the last few years, e.g., feedback linearization strategy [18] and passivity-based control methodology [21]. These proposed nonlinear design strategies present large complexity, so it is quite necessary to develop a control method that achieves system stability, desired performance, and simultaneously, easy to design.

Analysis and synthesis for switched systems have attracted increasing attention in the control community. Switched systems are comprised of a collection of subsystems together with a switching law that specifies the switching between the subsystems. Switched systems have a wide range of applications in the physical and engineering systems, which are mainly due to numerous practical systems exhibiting switched nature and the growing use of computers in the control of physical plants. In the aerospace field, many design problems can be viewed as the analysis and synthesis of the switched system, such as aircraft controller design, fault tolerant controller design, stability analysis of spacecraft formation, angle of attack and normal acceleration limiter design, and modeling and control of flow systems (see [27] and references therein).

Focusing on wide-range rapidly varying characteristic of the load and the background of industrial application, this paper proposed a switched control strategy for the VSR based on the concept of switched system. Several linear controllers are designed for different operating points of the VSR, and certain controllers are selected according to the load resistance value. The proposed control system is modeled by a sixth-order switched linear system, and stability of the system is analyzed

Manuscript received June 18, 2010; revised October 11, 2010; accepted November 13, 2010. Date of current version January 9, 2012. Recommended for publication by Associate Editor C. A. Canesin.

The authors are with the Beijing University of Aeronautics and Astronautics, Beijing 100191, China (e-mail: zhangw@asee.buaa.edu.cn; egibus@163.com; liuxinbo@asee.buaa.edu.cn; zhouyuanjun_buaa@263.net).

Color versions of one or more of the figures in this paper are available online at http://ieeexplore.ieee.org.

Digital Object Identifier 10.1109/TPEL.2010.2095507

0885-8993/$26.00 © 2011 IEEE

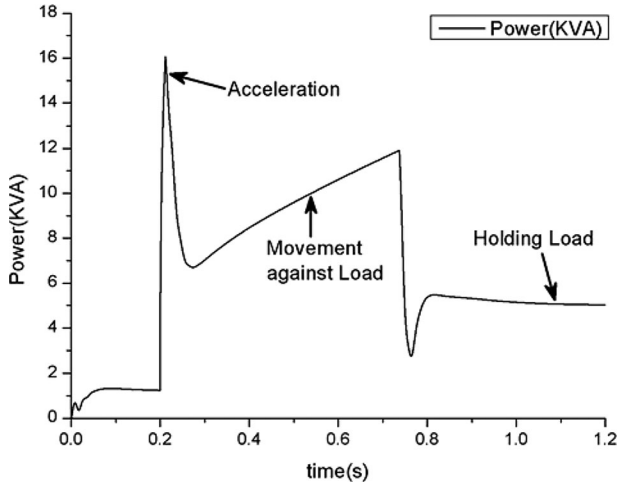

Fig. 1. Dynamic load profile.

by the common Lyapunov function method [28]. Compared with existing nonlinear control methods, the proposed switched control strategy is simpler. Compared with linear control methods, the proposed control strategy can guarantee system stability and desired performance under a wide-range rapidly varying load.

II. Characteristics of the Electric Actuator Load

A. Dynamic Nature of the Electric Actuator Load

The aircraft electric actuators that drive the movements of control surfaces of an aircraft are rapid position control systems. The actuator load demands a short term, high peak power with a fairly low steady state or background loading of less than 10% of the peak requirement. This obviously depends on the particular application, and it is usually called the dynamic load of the aircraft power grid.

Fig. 1 illustrates the dynamic nature of an electric actuator load as it moves a surface from rest at one position to rest at another position. There are three basic parts to the load cycle [29].

1) Input of power to accelerate the motor and inertia of the load.
2) Surface moving against the load (motor delivering speed and torque).
3) Surface holding the load (motor delivering torque but no speed).

From Fig. 1, it can be seen that the peak power of the electric actuator reaches about 16 kVA, which is more than ten times of the lowest power. In consequence, the actuator can be regarded as a large signal disturbance to the voltage source.

B. Constant Power Nature of the Electric Actuator Load

Generally speaking, the electric actuator is not a typical CPL because of the dynamic nature described in Section II-A. However, the system has the feedback control with the actuator position command supplied from a higher level control system of the aircraft. The feedback makes the system behave as a typical CPL in small time scales with small-signal negative resistance.

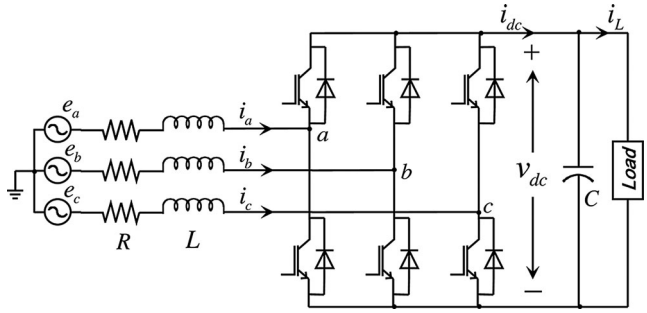

Fig. 2. AC/DC votage source PWM converter.

The value of the constant power drawn from the power source only depends on the operating point within the operating cycle. Hence, it can be treated as a special CPL. While an "ideal" CPL can be modeled as the standard nonlinear model ($i_L = P_L/v$), an electric actuator load can be expressed as $i_L = P(t)/v$. It means that i_L would rise correspondingly if the dc-bus voltage of the source falls with the rise of the output power, which may be a vicious circle for the power source.

In conclusion, both the dynamic nature and the constant power nature of an electric actuator make big challenges for the power source. In the following discussion, a switched controlled three-phase VSR with an "ideal" CPL, of which the dynamic response is the same as that shown in Fig. 1, is designed and analyzed.

III. Modeling of PWM Converters

A power circuit of the three-phase VSR is shown in Fig. 2. It is usually assumed that a resistive load R_L is connected to the output terminal [24]. An improved linear state-space modeling of a three-phase voltage source rectifier is [22]

$$\dot{i}_{qe} = -\frac{R}{L} i_{qe} - \omega i_{de} + \frac{1}{L}(e_{qe} - v_{qe}) \tag{1}$$

$$\dot{i}_{de} = -\frac{R}{L} i_{de} + \omega i_{qe} + \frac{1}{L}(e_{de} - v_{de}) \tag{2}$$

$$\dot{u} = -\frac{2}{R_L C} u + \frac{3e_{de}}{C} i_{de} + \frac{3e_{qe}}{C} i_{qe} \tag{3}$$

$$u = v_{\mathrm{dc}}^2 \tag{4}$$

where $e_{dq,e}, i_{dq,e}$, and $v_{dq,e}$ represent the source voltage, the current, and the rectifier input voltage in the synchronous $d-q$ reference frame, respectively,

R and L denote the line resistance and the input inductance, respectively,

ω is the source angular frequency,

v_{dc} is the dc-bus voltage, and

R_L is the load resistance.

Note that in this paper, a variable resistor $R(v_{\mathrm{dc}}, P_L)$ is employed in order to simulate the CPL characteristic of the electric actuator, and for a CPL we have

$$R(v_{\mathrm{dc}}, P_L) = \frac{v_{\mathrm{dc}}^2}{P_L} = \frac{u}{P_L} \tag{5}$$

where P_L denotes the load power.

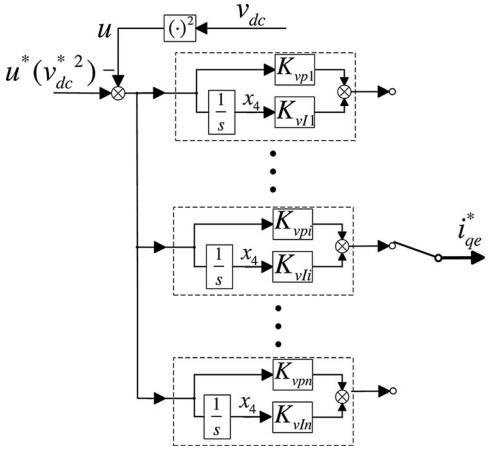

Fig. 3. Proposed dc-bus switched voltage regulator.

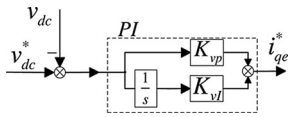

Fig. 4. Classical linear *PI* voltage controller.

Let $R(v_{\rm dc}, P_L)$ replace R_L in (3), and we get

$$\dot{u} = -\frac{2}{C}P_L + \frac{3e_{de}}{C}i_{de} + \frac{3e_{qe}}{C}i_{qe}. \tag{6}$$

Therefore, in this study, VSR under a CPL is modeled by (1), (2), (4), and (6).

In fact, in dc circuits, we have

$$P_L = v_{\rm dc} I_L \tag{7}$$

where i_L denotes the load current.

From (5) and (7), we get

$$R(v_{\rm dc}, P_L) = R(v_{\rm dc}, I_L) = \frac{v_{\rm dc}}{I_L}. \tag{8}$$

Therefore, $R(v_{\rm dc}, P_L)$ [or $R(v_{\rm dc}, I_L)$] is the input resistance (the apparent resistance of the load) that can be calculated by (8).

IV. Switched Control of VSRs

In this section, a novel switched control method for three-phase VSRs will be presented. The switched control method aims at well regulation of the dc-bus voltage of VSRs under a wide-range rapidly varying load.

A. Switched Control of the DC-Bus Voltage Regulator

Fig. 3 shows the structure of the proposed switched control method. Different from the classical linear *PI* voltage control scheme that is depicted in Fig. 4 [14], there are a set of *PI* subcontrollers in the voltage-switched control method. The gains of different *PI* subcontrollers correspond to different loads at the dc link. In this study, the apparent resistance $R(v_{\rm dc}, P_L)$ [or $R(v_{\rm dc}, I_L)$] is selected as the switching law that provides guidelines to select a proper *PI* subcontrollers when the load changes. Besides, *u* is considered as the state variable instead of the conventional state variable $v_{\rm dc}$ [22], [23]. The variable x_4 denotes the output of the integrator of the *PI* subcontroller. For a selected *PI* subcontroller *i*, the control law of the voltage controller is

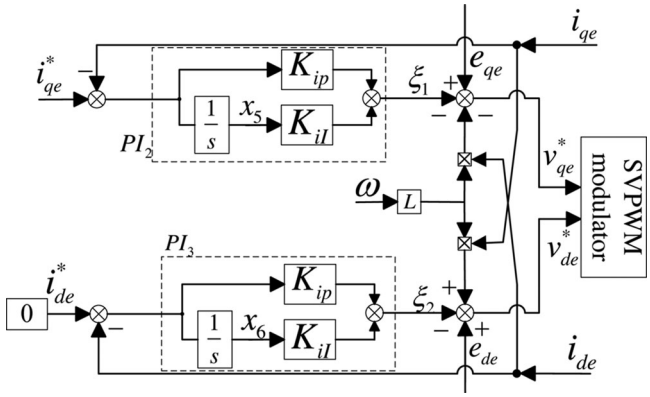

Fig. 5. Block diagram of the current controller with current forward feedback decoupling network.

$$i_{qe}^* = K_{vpi}(u^* - u) + K_{vIi}x_4, \quad i = 1, 2, \ldots, n \tag{9}$$

$$\dot{x}_4 = u^* - u \tag{10}$$

where *n* is the number of the subcontrollers.

B. Current Controller

The current controller that consists of two *PI* controllers (PI_2 and PI_3) is depicted in Fig. 5 [19], [25], [26]. In this control scheme, the cross-coupling terms of $\omega L i_{de}$ and $\omega L i_{qe}$ in (1) and (2) are compensated by feedforward at the last stage of the controller. In consequence, the *q*-axis current of i_{qe} that is the active current can be controlled independently on i_{de} and *u* (or $v_{\rm dc}^2$), so can the reactive current i_{de}. The variables of i_{de}^* and i_{qe}^* are the reference value of i_{de} and i_{qe}. For unit power factor when rectifying, i_{de}^* is zero and i_{qe}^* is set by the outer voltage controller. Let the variables x_5 and ξ_1 denote the output of the integrator of PI_2 and the output of PI_2, respectively, the control law of PI_2 is

$$\xi_1 = K_{ip}(i_{qe}^* - i_{qe}) + K_{iI}x_5 \tag{11}$$

$$\dot{x}_5 = i_{qe}^* - i_{qe}. \tag{12}$$

Similarly, the control law of PI_3 is given by

$$\xi_2 = K_{ip}(i_{de}^* - i_{de}) + K_{iI}x_6 \tag{13}$$

$$\dot{x}_6 = i_{de}^* - i_{de} \tag{14}$$

$$i_{de}^* = 0. \tag{15}$$

The control law of the current controller is

$$v_{qe}^* = -\xi_1 + e_{qe} - \omega L i_{de} \tag{16}$$

$$v_{de}^* = -\xi_2 + e_{de} + \omega L i_{qe}. \tag{17}$$

C. Closed-Loop Model of the System

Let $x = [i_{qe}, i_{de}, u, x_4, x_5, x_6]^T$ denote a state variable vector.

For different operating points $i \in \Omega = \{1, 2, ..., n\}$, different linear systems are first constructed.

$$\dot{x} = A_i x + b\mu, \qquad i \in \{1, 2, \ldots, n\}$$

$$A_i = \begin{bmatrix} -\frac{R+K_{ip}}{L} & 0 & -\frac{K_{ip}K_{vpi}}{L} & \frac{K_{ip}K_{vIi}}{L} & \frac{K_{iI}}{L} & 0 \\ 0 & -\frac{R+K_{ip}}{L} & 0 & 0 & 0 & \frac{K_{iI}}{L} \\ \frac{3e_{qe}}{C} & \frac{3e_{de}}{C} & 0 & 0 & 0 & 0 \\ 0 & 0 & -1 & 0 & 0 & 0 \\ -1 & 0 & -K_{vpi} & K_{vIi} & 0 & 0 \\ 0 & -1 & 0 & 0 & 0 & 0 \end{bmatrix} \tag{18}$$

$$b\mu = \left[-\frac{K_{iqp}K_{vpi}}{L}u^*, 0, -\frac{2P_L}{C}, u^*, K_{vpi}u^*, 0 \right]^T. \tag{19}$$

The detailed derivation is shown in the Appendix.

By selecting $R(v_{\rm dc}, P_L)$ (or $R(v_{\rm dc}, I_L)$) R_L as the switching law $\sigma(t) \to \Omega = \{1, 2, \ldots, n\}$, a switched linear system associated with the proposed switched control scheme is achieved as follows:

$$\dot{x} = A_{\sigma(t)}x + b\mu. \tag{20}$$

By assuming that the synchronous $d-q$ reference frame is aligned with the phase-A voltage of the supply, the $d-q$ components of the source voltage are expressed as

$$\begin{cases} e_{de} = 0 \\ e_{qe} = E_m \end{cases} \tag{21}$$

where E_m denotes the amplitude of the phase voltage.

D. Stability Analysis

In Section IV-C, the switched control scheme has been described by a switched linear system. In the sequel, the stability analysis of such control scheme is performed by the common Lyapunov function method.

Theorem 1: If there exist a positive definite matrix P, such that linear matrix inequalities (LMIs)

$$A_i^T P + PA_i < 0 \tag{22}$$

hold for every $i \in \Omega$, then under arbitrary switching law, the closed-loop switched linear system (20) is input-to-state uniformly bounded.

Proof: If linear matrix inequalities (22) hold, it can be readily verified that $V(t) = x^T Px$ is a common Lyapunov function for the autonomous switched linear system $\dot{x} = A_{\sigma(t)}x$. Thus, the system $\dot{x} = A_{\sigma(t)}x$ is globally uniformly asymptotically stable under arbitrary switching law [28].

Considering that the globally uniformly asymptotical stability means that the globally uniformly exponential stability for switched linear systems [28], by Lemma 1 in [30], it can be concluded that the closed-loop switched system (20) is input-to-state uniformly bounded under any switching law $\sigma(t)$.

TABLE I
SPECIFICATIONS OF THREE-PHASE PWM BOOST RECTIFIER

Parameters Setting	Value
Source voltage E_m (RMS)	115V
DC-bus voltage v_{dc}	270V
Line inductor L	0.5mH
Inductor resistance R	0.2 Ω
DC-bus capacitor C	2000uF
Line frequency ω	800 π rad/s
PWM carrier frequency	16kHz

Remark 1: In this study, the linear matrix inequality (22) is solved by the related LMI commands in Robust Control Toolbox of MATLAB R2007a. The programing is easy and the readers who are interested in solving LMIs are recommended to read the help documents of MATLAB R2007a.

V. SIMULATION AND EXPERIMENTAL RESULTS

This section applies the proposed switched control method to design a VSR for an aircraft ac–dc converter in accordance with the requirements of the HVdc system stated in MIL-STD-704 F. The VSR was employed on an aircraft electric actuator that is a fast dynamic load. Simulation and experimental results are presented.

A. Requirements of the System

A simulation system model based on Fig. 2 is constructed with the specifications listed in Table I. According to the requirement of MIL-STD-704 F, normal steady voltage transient of the 270 V dc system shall be within the envelope of 280 and 250 V, and ripple amplitude of the steady voltage should be less than 6 V.

B. Design of the Switched Controller

Since $v_{\rm dc}$ and i_L are measured by sensors, the apparent $R(v_{\rm dc}, P_L)$[or $R(v_{\rm dc}, I_L)$] that is the switching law of the voltage controller, is calculated by (8). In this study, its variety range is mainly within (4–95 Ω). Then, the range (4–95 Ω) is divided into three switching subranges (hence, we have n =3). The parameters K_{ip}, K_{iI}, K_{vpi}, and K_{vIi} are listed in Table II. Subcontroller 1, associated with $R(v_{\rm dc}, P_L) = (28\ \Omega, +\infty)$, is selected when a low power load is connected. Subcontroller 2, corresponding to $R(v_{\rm dc}, P_L) = (5\ \Omega, 28\ \Omega)$, which is chosen when a middling load is connected, is the main controller, because the load R_L varies mainly in the range of (5–28 Ω). Subcontroller 3, associated with $R(v_{\rm dc}, P_L) = (0\ \Omega, 5\ \Omega]$, is

TABLE II
PI PARAMETERS OF THE CURRENT CONTROLLER AND SWITCHED VOLTAGE CONTROLLER

Current controller	$K_{ip} = 20$	$K_{iI} = 50$	
Subcontroller 1:	$K_{vp1} = 0.002$	$K_{vI1} = 0.03$	$R_L \in (28, +\infty)$
Subcontroller 2:	$K_{vp2} = 0.005$	$K_{vI2} = 0.10$	$R_L \in (5, 28]$
Subcontroller 3:	$K_{vp3} = 0.02$	$K_{vI3} = 0.10$	$R_L \in (0, 5]$

selected when the peak power takes place. The proportional coefficient of the subcontroller 3 is chosen large enough to achieve rapid response.

C. Stability Analysis

Substituting the parameters listed in Tables I and II into matrix A_i of (18), it gives

$$A_1 = 1.0 \times 10^5 \times \begin{bmatrix} -0.404 & 0 & -0.0008 & 0.004 & 1.0 & 0 \\ 0 & -0.404 & 0 & 0 & 0 & 1.0 \\ 1.725 & 0 & 0 & 0 & 0 & 0 \\ 0 & 0 & -0.00001 & 0 & 0 & 0 \\ -0.00001 & 0 & -0.00000002 & 0.0000001 & 0 & 0 \\ 0 & -0.00001 & 0 & 0 & 0 & 0 \end{bmatrix}$$

$$A_2 = 1.0 \times 10^5 \times \begin{bmatrix} -0.404 & 0 & -0.0024 & 0.04 & 1 & 0 \\ 0 & -0.404 & 0 & 0 & 0 & 1 \\ 1.725 & 0 & 0 & 0 & 0 & 0 \\ 0 & 0 & -0.00001 & 0 & 0 & 0 \\ -0.00001 & 0 & -0.00000006 & 0.000001 & 0 & 0 \\ 0 & -0.00001 & 0 & 0 & 0 & 0 \end{bmatrix}$$

$$A_3 = 1.0 \times 10^5 \times \begin{bmatrix} -0.404 & 0 & -0.008 & 0.04 & 1 & 0 \\ 0 & -0.404 & 0 & 0 & 0 & 1 \\ 1.725 & 0 & 0 & 0 & 0 & 0 \\ 0 & 0 & -0.00001 & 0 & 0 & 0 \\ -0.00001 & 0 & -0.0000002 & 0.000001 & 0 & 0 \\ 0 & -0.00001 & 0 & 0 & 0 & 0 \end{bmatrix}.$$

The three matrixes A_1, A_2, and A_3 are Hurwitz stable. Further, there exists a positive definite matrix $P = 1.0 \times 10^8$ as shown at the bottom of this page, satisfying the linear matrix inequalities (22) such that the closed-loop switched system, corresponding to the switched control system for VSR, has a common Lyapunov function and thus it is uniformly input-to-state bounded under arbitrary switching law.

D. Simulation Results

The rectifier system specified in Section V-B is modeled in MATLAB/simulink with the aircraft electric actuator load shown in Fig. 1. For the purpose of comparison, simulations are performed for the proposed switched control scheme and the classical linear *PI* control scheme (the second dc-voltage control method in [14]). The parameters of the three linear *PI* voltage controllers PI_1, PI_2, and PI_3, are the same as subcontroller 1, subcontroller 2, and subcontroller 3 listed in Table II. The responses of the switched controller and the three linear *PI* controllers PI_1, PI_2, and PI_3 are depicted in Fig. 6.

Fig. 6(a) shows the response of the linear *PI* controller PI_1. The starting-up response is smooth and fast with a small overshoot. However, the dc-bus voltage drops down to zero abruptly as the load current climbs up rapidly, when the motor and load inertia accelerates.

Fig. 6(b) shows the response of the linear *PI* controller PI_2. Although the system could maintain stability during the whole dynamic process, the dc-bus voltage falls obviously to about 229 V when the peak power occurs and increases to about 285 V when the load power drops. Therefore, the disturbance rejection ability of this controller is weak and it cannot meet the normal voltage transient requirements of MIL-STD-706 F.

Fig. 6(c) shows the response of the linear *PI* controller PI_3. Due to the large proportional gain of the controller, only small dip and peaking in output voltage are observed. However, there exist too many undesirable oscillations from 0.5 to 0.7 s. The maximum ripple voltage is larger than 6 V. Thus, the response cannot meet the ripple amplitude requirement of MIL-STD-706 F. Furthermore, a big overshoot appears in power-up situations.

$$P = 1.0 \times 10^8 \times \begin{bmatrix} 0.000026 & 0 & 0.0000002 & -0.00000144 & -0.0000892 & 0 \\ 0 & 0.00005929 & 0 & 0 & 0 & -0.0000202 \\ 0.0000002 & 0 & 0.00000006 & -0.0000005 & -0.0000149 & 0 \\ -0.00000144 & 0 & -0.000000483 & 0.00020771 & 0.00615297 & 0 \\ -0.0000892 & 0 & -0.00001491 & 0.006153 & 6.68481867 & 0 \\ 0 & -0.00002023 & 0 & 0 & 0 & 6.456299 \end{bmatrix}$$

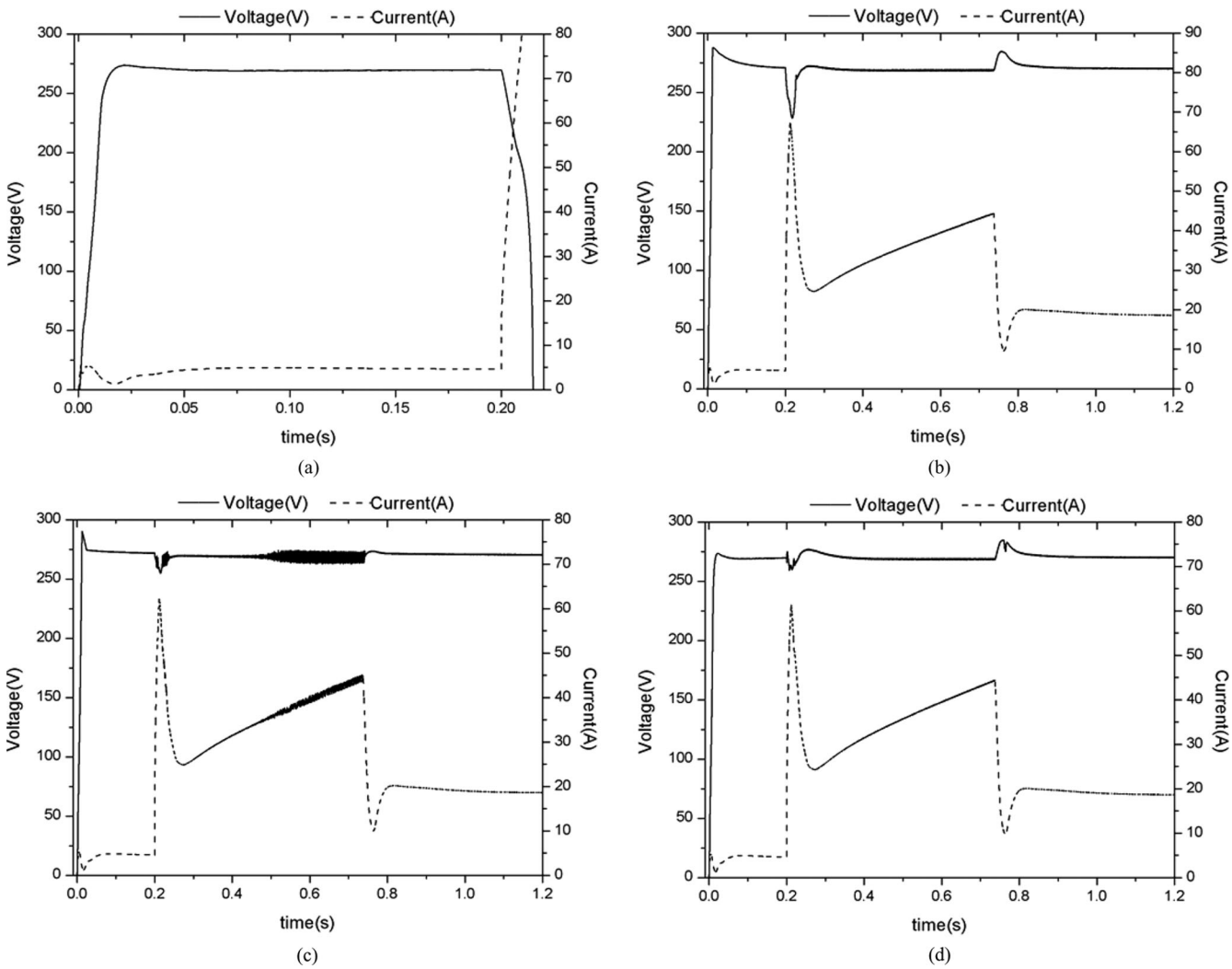

Fig. 6. Responses of (a) classical linear *PI* controller PI_1, (b) classical linear *PI* controller PI_2, (c) classical linear *PI* controller PI_3, and (d) switched voltage controller with the CPL.

Fig. 6(d) shows the response of the proposed switched controller. It can be seen that a balanced and optimized dc-bus response, which has an acceptable small ripple, little oscillations during the dynamic process, and a neglectable small overshoot in power-up situations, is achieved. The dc-bus voltage falls to 259 V at the peak load power and the largest overshoot appears at 0.76 s to about 280 V when the load current drops. Therefore, the system controlled by the switched control method meets the requirements of MIL-STD-704 F.

E. Experimental Results

A prototype of the three-phase PWM rectifier, as shown in Fig. 7, has been developed and some experimental tests have been carried out. The configuration and the parameters of the experimental system are the same as the simulation model. A three-phase 400-Hz power source was used as the voltage supply, and three 0.5-mH line inductors are connected between the supply and the rectifier. The rating of the used three-phase IGBT module (PM100CSA120) is 100 A/1200 V. A 2000 μF/450 V aluminum electrolytic capacitor is placed across dc bus. A DSP (TMS320F2812) is selected as the core controller. The supply phase voltage is set to 115 V and the dc-bus voltage is set to be 270 V. PWM-carrying frequency is set to be 16 kHz. A 10-kW electric actuator prototype, as shown in Fig. 8, is used as the active load of the rectifier. Hall voltage sensors and hall current sensors are used to measure the ac- and dc-side voltage and current.

The VSR under the proposed switched controller and two linear *PI* controllers (controller 1 and controller 2 correspond to subcontroller 2 and subcontroller 3 in Section V-B, respectively) is studied experimentally and shown in Figs. (9)–(11). In case of unsafety of large current, experiments on subcontroller 1 were not done. Fortunately, the results are obvious because the small proportional gain cannot handle the dynamic load. Fig. 9(a) shows the experimental dc bus dynamic response of the system under switched voltage controller. It can be seen that there are only small ripples in the dc-bus voltage during the whole dynamic process of the actuator. Fig. 9(b) illustrates the experimental dc-bus dynamic response of the system for a linear *PI* controller 1, the parameters of which is the same as the subcontroller 2 in Section V-B. It can be seen in Fig. 9(b) that there

Fig. 7. Prototype of the PWM rectifier.

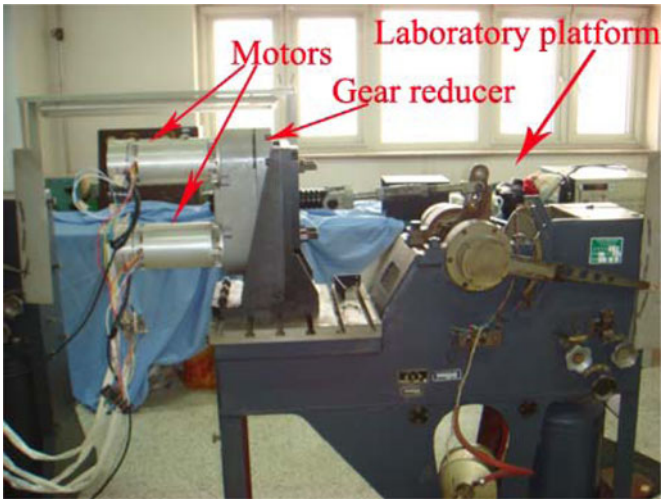

Fig. 8. Ten-kilowatt electric actuator and laboratory platform.

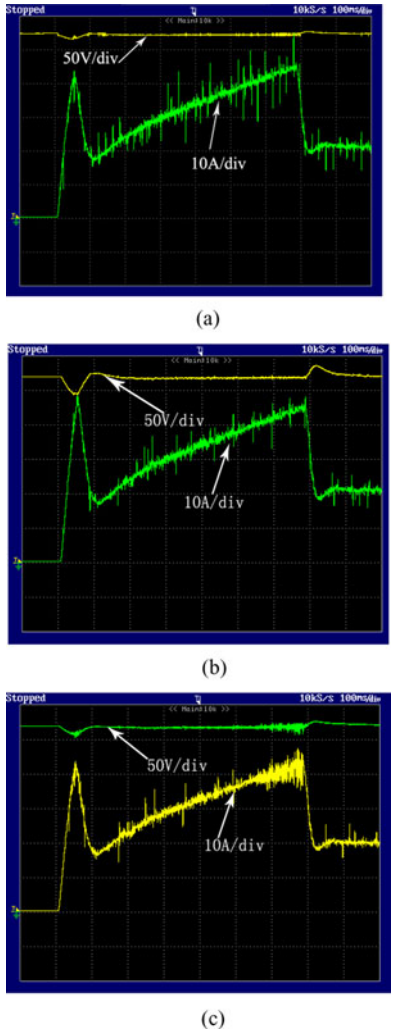

Fig. 9. Experimental results: dc-link voltage and load current for (a) switched voltage controller; (b) linear *PI* voltage controller 1; (c) linear *PI* voltage controller 2.

is a huge dip of about 30 V when the peak load power occurs and a big overshoot of about 15 V when the load power drops on the dc-bus voltage. Fig. 9(c) illustrates the experimental dc-bus dynamic response of the system for a linear *PI* controller 2, the parameters of which is the same as the subcontroller 2 in Section V-B. It can be seen in Fig. 9(c) that undesirable oscillations appear in the dc voltage, and it leads to oscillations in the load current because of the CPL characteristic.

In steady state, the switched controller can achieve high power factor and low total harmonic distortion (THD) on the ac side. The input waveforms of phase-A in the ac side of the rectifier under switched voltage controller are shown in Fig. 10. It can be seen from Fig. 10(a) that the input power factor is almost unity in steady state. Fourier analysis of this current shows that the THD is 1.35%. In fact, the switched controller performs like a linear *PI* controller in steady state due to the switching law.

The transient input current and voltage waveforms are shown in Fig. 11. Fig. 11(a) shows the source voltage and input current of phase-A in transient state for the switched voltage controller. It can be seen that the power factor and THD are slightly influenced. Fig. 11(b) shows the source voltage and input current of phase-A in transient state for the *PI* controller 1. It can be seen that the power factor is influenced more seriously than that in Fig. 11(a). Fig. 11(c) shows the source voltage and input current of phase-A in transient state for the *PI* controller 2. It can be seen that the power factor and THD are influenced seriously.

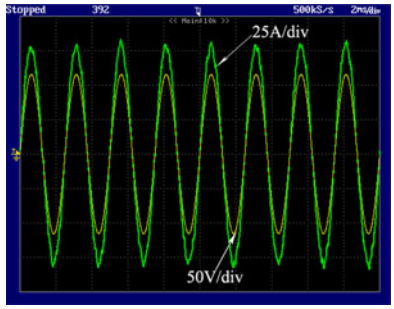

Fig. 10. Experimental results: source voltage and input current of phase-A in steady state for switched control method.

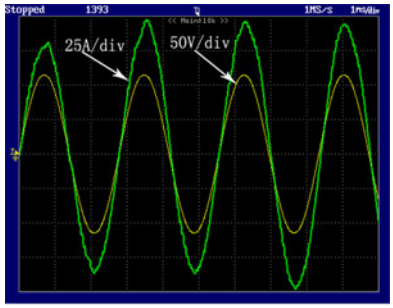

(a)

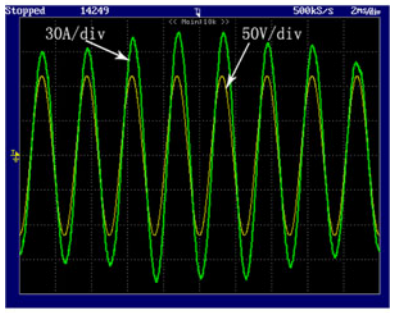

(b)

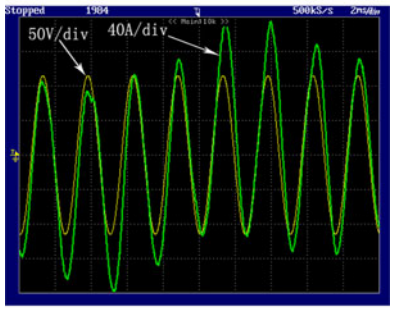

(c)

Fig. 11. Experimental results: source voltage and input current of phase-A in transient state for (a) switched voltage controller; (b) linear *PI* voltage controller 1; and (c) linear *PI* voltage controller 2.

In fact, the input performance and the output performance of the VSR are coincident. The big drop on the dc bus in Fig. 9(b) responds to the decrease of the power factor on the ac side in Fig. 11(b), and the big oscillations on the dc bus in Fig. 9(c) respond to the decrease of the power factor and THD on the ac side in Fig. 11(b). Under switched voltage controller, the dc-bus voltage is regulated better in transient state, so are the power factor and THD of the ac side. Experimental results show that the performances of the proposed system comply with the MIL-STD-704 F requirements.

F. Discussion

The simulation results and experimental results show that the proposed switched control method has a desirable capacity of regulating dc-bus voltage with a wide-range rapidly varying dynamic load, such as the electric actuator. Based on the proposed method, a more than 50% reduction in the dip of the dc-bus voltage and a 40% reduction in the overshoot of the dc-bus voltage are achieved compared with the classical linear *PI* VOC principle. At the same time, the input current power factor and THD of the ac side are improved in transient state.

VI. Conclusion

In this paper, a new switched control method is introduced to control the VSR. The proposed switched voltage control approach could provide a simple, effective way to overcome the problem of wide-range load regulation. Several linear controllers are designed according to the derived switched voltage controller for the VSR at different operating points and a certain controller is selected by the apparent load resistance value. To achieve better responses, one can increase the number of subcontrollers of the switched regulator reasonably. Based on the concept of switched system, the stability of the proposed control scheme can be attained. Simulation and experimental results of a switched controlled VSR with an electric actuator load show that the presented switched control method has a desirable capacity of regulating dc-bus voltage with such wide-range rapidly varying dynamic load.

Appendix

From (1) to (17), the control law of the system can be obtained as follows.

Substituting (9) back into (11) and (12) yields two new equations as

$$\xi_1 = K_{iqp}(K_{vpi}(u^* - u) + K_{vIi}x_4 - i_{qe}) + K_{iqI}x_5 \quad \text{(A1)}$$

$$\dot{x}_5 = K_{vpi}(u^* - u) + K_{vIi}x_4 - i_{qe}. \quad \text{(A2)}$$

Substituting (15) back into (13) and (14) yields two new equations as

$$\xi_2 = -K_{idp}i_{de} + K_{idI}x_6 \quad \text{(A3)}$$

$$\dot{x}_6 = -i_{de}. \quad \text{(A4)}$$

Substituting (A1) back into (16) yields the q-axis control output

$$v_{qe}^* = -(K_{iqp}(K_{vpi}(u^* - u) + K_{vIi}x_4 - i_{qe}) + K_{iqI}x_5) + e_{qe} - \omega L i_{de}. \quad \text{(A5)}$$

Substituting (A3) back into (17) yields the d-axis control output

$$v_{de}^* = -(-K_{idp}i_{de} + K_{idI}x_6) + e_{de} + \omega L i_{qe}. \quad \text{(A6)}$$

Considering the ideal condition, the effects of harmonics, saturation, and transistor turnoff delays are neglected. In consequence, the (A7) and (A8) are satisfied.

$$v_{qe} = v_{qe}^* \quad \text{(A7)}$$

$$v_{de} = v_{de}^*. \quad \text{(A8)}$$

From (A5) to (A8), we get

$$v_{qe} = -(K_{iqp}(K_{vpi}(u^* - u) + K_{vIi}x_4 - i_{qe}) + K_{iqI}x_5) + e_{qe} - \omega L i_{de} \quad \text{(A9)}$$

$$v_{de} = -(-K_{idp}i_{de} + K_{idI}x_6) + e_{de} - \omega L i_{qe}. \quad \text{(A10)}$$

Substituting (A9) back into (1) and (A10) back into (2), the closed-loop equations of the system that can be rearranged in the following form are yielded:

$$\dot{i}_{qe} = -\frac{R+K_{iqp}}{L} i_{qe} - \frac{K_{iqp}K_{vpi}}{L} u + \frac{K_{iqp}K_{vIi}}{L} x_4 + \frac{K_{iqI}}{L} x_5 - \frac{K_{iqp}K_{vpi}}{L} u^* \tag{A11}$$

$$\dot{i}_{de} = -\frac{R+K_{idp}}{L} i_{de} + \frac{K_{idI}}{L} x_6. \tag{A12}$$

Let $x = [i_{qe}, i_{de}, u, x_4, x_5, x_6]^T$ denote state variable vector. From the aforementioned analysis, (6), (10), (A2), (A4), (A11), and (A12) can be rearranged in the form of $\dot{x} = A_i x + b\mu$, $i \in \{1, 2, \ldots, n\}$, where

$$A_i = \begin{bmatrix} -\frac{R+K_{iqp}}{L} & 0 & -\frac{K_{iqp}K_{vpi}}{L} & \frac{K_{iqp}K_{vIi}}{L} & \frac{K_{iqI}}{L} & 0 \\ 0 & -\frac{R+K_{idp}}{L} & 0 & 0 & 0 & \frac{K_{idI}}{L} \\ \frac{3e_{qe}}{C} & \frac{3e_{de}}{C} & 0 & 0 & 0 & 0 \\ 0 & 0 & -1 & 0 & 0 & 0 \\ -1 & 0 & -K_{vpi} & K_{vIi} & 0 & 0 \\ 0 & -1 & 0 & 0 & 0 & 0 \end{bmatrix}$$

$$b\mu = \left[-\frac{K_{iqp}K_{vpi}}{L} u^*, 0, -\frac{2P_L}{C}, u^*, K_{vpi}u^*, 0 \right]^T.$$

ACKNOWLEDGMENT

The authors would like to thank the reviewers for their valuable suggestions that enable them to clarify the analysis and improve the readability of this paper.

REFERENCES

[1] J. R. Rodriguez, J. W. Dixon, J. R. Espinoza, J. Pontt, and P. Lezana, "PWM regenerative rectifiers: State of the art," *IEEE Trans. Ind. Electron.*, vol. 52, no. 1, pp. 5–22, Feb. 2005.

[2] R. Ghosh and G. Narayanan, "Control of three-phase, four-wire PWM rectifier," *IEEE Trans. Power Electron.*, vol. 23, no. 1, pp. 96–106, Jan. 2008.

[3] J. A. Rosero, J. A. Ortega, E. Aldabas, and L. Romeral, "Moving towards a more electric aircraft," *IEEE Aerosp. Electron. Syst. Mag.*, vol. 22, no. 3, pp. 3–9, Mar. 2007.

[4] A. Garcia, J. Cusido, J. A. Rosero, J. A. Ortega, and L. Romeral, "Reliable electromechanical actuators in aircraft," *IEEE Aerosp. Electron. Syst. Mag.*, vol. 23, no. 8, pp. 19–25, Aug. 2008.

[5] G. Gong, M. L. Heldwein, U. Drofenik, J. Minibock, K. Mino, and J. W. Kolar, "Comparative evaluation of three-phase high-power-factor AC-DC converter concepts for application in future more electric aircraft," *IEEE Trans. Ind. Electron.*, vol. 52, no. 3, pp. 727–737, Jun. 2005.

[6] Y. Guo, X. Wang, H. C. Lee, and B.-T. Ooi, "Pole-placement control of voltage-regulated PWM rectifiers through real-time multiprocessing," *IEEE Trans. Ind. Electron.*, vol. 41, no. 2, pp. 224–230, Apr. 1994.

[7] R. Wu, S. B. Dewan, and G. R. Slemon, "A PWM AC-to-DC converter with fixed switching frequency," *IEEE Trans. Ind. Applicat.*, vol. 26, no. 5, pp. 880–885, Sep./Oct. 1990.

[8] J. W. Dixon and B. T. Ooi, "Indirect current control of a unity power factor sinusoidal current boost type three phase rectifier," *IEEE Trans. Ind. Electron.*, vol. 35, no. 4, pp. 508–515, Nov. 1988.

[9] B. Yin, R. Oruganti, S. K. Panda, and A. K. S. Bhat, "An output-power-control strategy for a three-phase PWM rectifier under unbalanced supply conditions," *IEEE Trans. Ind. Electron.*, vol. 55, no. 5, pp. 2140–2151, May 2008.

[10] X. H. Wu, S. K. Panda, and J. X. Xu, "DC link voltage and supply-side current harmonics minimization of three phase PWM boost rectifiers using frequency domain based repetitive current controllers," *IEEE Trans. Power Electron.*, vol. 23, no. 4, pp. 1987–1997, Jul. 2008.

[11] A. Bouafia, J.-P. Gaubert, and F. Krim, "Predictive direct power control of three-phase pulsewidth modulation (PWM) rectifier using space-vector modulation (SVM)," *IEEE Trans. Power Electron.*, vol. 25, no. 1, pp. 228–236, Jan. 2010.

[12] X. H. Wu, S. K. Panda, and J. X. Xu, "Analysis of the instantaneous power flow for three-phase PWM boost rectifier under unbalanced supply voltage conditions," *IEEE Trans. Power Electron.*, vol. 23, no. 4, pp. 1679–1691, Jul. 2008.

[13] A. Draou, Y. Sato, and T. Kataoka, "A new state feedback based transient control of PWM AC to DC voltage type converters," *IEEE Trans. Power Electron.*, vol. 10, no. 6, pp. 716–724, Nov. 1995.

[14] P. Verdelho and G. D. Marques, "DC voltage control and stability analysis of PWM voltage-type reversible rectifiers," *IEEE Trans. Ind. Electron.*, vol. 45, no. 2, pp. 263–273, Apr. 1998.

[15] M.-T. Tsai and W. I. Tsai, "Analysis and design of three-phase AC-to-DC converters with high power factor and near-optimum feedforward," *IEEE Trans. Ind. Electron.*, vol. 46, no. 3, pp. 535–543, Jun. 1999.

[16] V. Blasko and V. Kaura, "A new mathematical model and control of a three-phase AC-DC voltage source converter," *IEEE Trans. Power Electron.*, vol. 12, no. 1, pp. 116–123, Jan. 1997.

[17] H. Komurcugil and O. Kukrer, "Lyapunov-based control for three phase PWM AC/DC voltage-source converters," *IEEE Trans. Power Electron.*, vol. 13, no. 5, pp. 801–813, Sep. 1998.

[18] D.-C. Lee, G.-M. Lee, and K.-D. Lee, "DC-bus voltage control of three-phase AC/DC PWM converters using feedback linearization," *IEEE Trans. Ind. Appl.*, vol. 36, no. 3, pp. 826–833, May/Jun. 2000.

[19] D.-C. Lee, "Advanced nonlinear control of three-phase PWM rectifiers," *Proc. IEE—Elect. Power Appl.*, vol. 147, no. 5, pp. 361–366, Sep. 2000.

[20] T.-S. Lee, "Input-output linearization and zero-dynamics control of three-phase AC/DC voltage-source converters," *IEEE Trans. Power Electron.*, vol. 18, no. 1, pp. 11–22, Jan. 2003.

[21] T.-S. Lee, "Lagrangian modeling and passivity-based control of three-phase AC/DC voltage source converters," *IEEE Trans. Ind. Electron.*, vol. 51, no. 4, pp. 892–902, Aug. 2004.

[22] Y. Ye, M. Kazerani, and V. H. Quintana, "A novel modeling and control method for three-phase PWM converters," in *Proc. 32nd Power Electron. Spec. Conf.*, Jun. 17–22,, 2001, vol. 1, pp. 102–107.

[23] Y. Ye, M. Kazerani, and V. H. Quintana, "Modeling, control and implementation of three-phase PWM converters," *IEEE Trans. Power Electron.*, vol. 18, no. 3, pp. 857–864, May 2003.

[24] A. W. Green, J. T. Boys, and G. F. Gates, "Three-phase voltage sourced reversible rectifier," *IEE Proc. Electric Power Appl.*, vol. 135, no. 6, pp. 362–370, 1988.

[25] M. Cichowlas and M. P. Kazmierkowski, "Comparison of current control techniques for PWM rectifiers," in *Proc. IEEE Int. Symp. Ind. Electron.*, Jul. 2002, vol. 4, pp. 1259–1263.

[26] H. Sugimoto, S. Moritomo, and M. Yano, "A high performance control of a voltage-type PWM converter," in *Proc. Conf. Rec. IEEE Power Electron. Spec. Conf. (PESC'88)*, Apr., pp. 360–368.

[27] Y. Z. Hou, C. Y. Dong, and Q. Wang, "Stability analysis of switched linear systems with locally overlapped switching law," *J. Guid., Control, Dyn.*, vol. 33, no. 2, pp. 396–403, 2010.

[28] D. Liberzon, *Switching in Systems and Control*. Boston, MA: Birkhäuser, 2003.

[29] D. R. Trainer and C. R. Whitley, "Electric actuation—Power quality management of aerospace flight control systems," in *Proc. IEE Int. Conf. Power Electron., Machines Drives*, 2003, pp. 229–234.

[30] J. P. Hespanha and A. S. Morse, "Stability of switched systems with average dwell-time," in *Proc. 38th Conf. Decision Control*, Phoenix AZ, 1999, pp. 2655–2660.

Wei Zhang was born in China, in 1982. He received the Bachelor's degree in electric engineering from the Beijing University of Aeronautics and Astronautics, Beijing, China, in 2006, where he is currently working toward the Ph.D. degree at Power Electronics and Power Drives Laboratory, School of Automation Science and Electrical Engineering.

His current research interests include motor drives, power converters, and control theory applications.

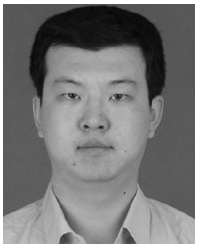

Yanze Hou received the Bachelor's degree in automation control from Northwestern Polytechnical University, Xi'an, China, in 2006. he is currently working toward the Ph.D. degree from the School of Automation Science and Electrical Engineering, Beijing University of Aeronautics and Astronautics, Beijing, China.

He is currently with Intelligent Control Laboratory, Beijing University of Aeronautics and Astronautics. His current research interests include switched system, adaptive control, and flight control.

Xinbo Liu received the B.S. degree in electrical engineering from the Beijing University of Aeronautics and Astronautics, Beijing, China, in 2005, where she is currently working toward the Ph.D. degree from Power Electronics and Power Drives Laboratory, Department of Automation Science and Electrical Engineering, Beijing University of Aeronautics and Astronautics, in the field of power electronics and stability analysis.

Yuanjun Zhou was born in China, in 1951. She received the Bachelor's and Master's degrees in electric engineering from Beijing University of Aeronautics and Astronautics, Beijing, China, in 1976 and 1982, respectively.

She was a visiting scholar at Kyoto University, Japan, from 1986 to 1988. She is currently a Full Professor of Electrical Engineering at Beijing University of Aeronautics and Astronautics, Beijing, China. She is the author of several books and papers. Her research interests include motor drives, power converters, and redundant mechanical and electrical control systems.